

Gold Nanoparticle Deposited on Screen-Printed Carbon Electrode for Electrochemical Detection of Nicotine in E-cigarette

Amirul Aiman Ali Amran¹, Lim Ying Chin¹, Nurasyiqin Azman¹, Nurfadhilah Jafar¹, Yusairie Mohd¹, Rosminazuin Ab Rahim^{2*}, Anis Nurashikin Nordin² and Zainiharyati Mohd Zain^{1*}

¹Electrochemical Material and Sensor (EMaS) Research Group, Faculty of Applied Sciences, Universiti Teknologi MARA, 40450 Shah Alam, Selangor, Malaysia

²MEMS-VLSI Research Unit, Department of Electrical and Computer Engineering, Engineering Faculty, International Islamic University Malaysia, 53100 Kuala Lumpur, Malaysia

*Corresponding author (e-mail: zainihar@uitm.edu.my)

Nicotine addiction is a global health problem that causes 4.9 million deaths each year. Nicotine addiction from smoking tobacco may harm both active and passive smokers. Due to nicotine's slow electrode kinetics and redox response occurring at positive potentials, there has been a need in designing electrode material for narrowing the electrochemical window for nicotine redox reaction on the current-potential curve. Nicotine oxidation happens at a higher potential making the signal susceptible to interference from oxygen, thus causing inconsistency in the electrochemical signal. Numerous electrode modifications have been attempted to solve the problem of nicotine's substantial overpotential on bare carbon electrodes. In this work, nicotine in e-cigarette tobacco products was detected using gold nanoparticles electrodeposited on screen-printed carbon electrode (AuNPs-SPCE). The gold solution was prepared from a precursor solution of 10 mM chloroauric acid, HAuCl₄. The screen-printed carbon electrode (SPCE) was immersed in the gold solution and was selectively electrodeposited on the SPCE surface at a potential of +0.53 V as the first layer deposition by using chronoamperometry (CA). Then, CA was performed at a constant potential of -0.9 V for approximately 900 seconds on the SPCE surface, resulting in a second layer with gold nanostructures. The gold nanostructures were characterised by using Scanning Electron Microscopy (SEM) and Elemental Dispersive X-ray Spectroscopy (EDX). The electrochemical analysis was proceeded using the fabricated AuNPs-SPCE as the working electrode in potassium ferrocyanide, K₄Fe(CN)₆, standard nicotine in 0.1 M PBS (pH 7), and liquid-flavoured e-cigarette (sample) using the cyclic voltammetry (CV) method. The effectiveness of the AuNPs-SPCE shows the detection of nicotine at a potential +0.2 V focusing on nicotine's oxidation peak. The oxidation peak calibration graph was linear from 0.00025 M to 0.03 M, with a correlation coefficient (R²) of 0.9920 and a limit detection of 8.3 mM within 2 secs of response time. This preliminary finding can contribute to the health care community in diagnosing nicotine addiction at an early stage to prevent tragic nicotine overdoses.

Keywords: Nicotine; electrochemical sensor; gold nanoparticle; electrodeposition, vape

Received: November 2022; Accepted: January 2023

Consumption of tobacco products can result in nicotine addiction and cause a variety of adverse health outcomes for both active and passive consumers of the burning tobacco products. Approximately 4.9 million deaths per year worldwide were reported due to consuming tobacco products [1]. Nicotine addiction has become a growing global health issue.

Nicotine is the common name to its chemical name of 3-(1-methyl-2-pyrrolidinyl) pyridine, as shown in Figure 1. It is a derivative of an alkaloid family. Nicotine is a compound that contains nitrogen, which can be discovered in tobacco leaves. It consists of 95% of purine alkaloid with strong addictive potential. Tobacco products are more addictive than other narcotics, such as cocaine and heroin, since they are

readily available on the market. It is also more well-known for its use as a natural repellent in agriculture and an anti-parasite in veterinary medicine, dietary nicotine, and fertiliser rather than for medicinal and pharmaceutical purposes [2].

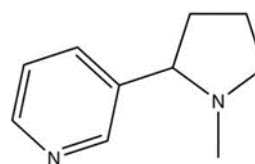


Figure 1. Nicotine 3-(1-methyl-2-pyrrolidinyl) pyridine. Source of structural formula [3].

Christopher Columbus was the first person who discovered the tobacco plant in America. America is the native of the tobacco plant and has become a medication and stimulant in their daily lives for at least 2,000 years ago. Tobacco herbs from the genus *Nicotiana*, such as *N. glauca*, *N. rustica*, *N. silvestris*, or *N. tabacum*, which naturally occur in the form of the S-(-) isomer [1]. Nicotine is an oily pale-yellow solution that is easily soluble in water at ambient temperature. In 1828, nicotine was identified as a poison compound from the first isolated nicotine from the tobacco leaves discovered by Wilhelm Heinrich Posselt, a doctor; and Karl Ludwig Reimann, a scientist, both from Germany. In the 19th century, people realised nicotine was poisonous and harmful to the community. Several countries have invented laws prohibiting the sale of nicotine in shops, including Malaysia; for example, it is illegal to sell cigarettes to underage in Malaysia.

With an estimated 1.3 billion dollars in sales in 2020, cigarettes were by far the most profitable tobacco product in Malaysia. 1.2 billion dollars will be the segment's revenue by 2025, according to the Consumer Market Outlook by Statista. By 2025, 19.6% of Malaysians are predicted to smoke, falling short of the country's objective of 15% set out in its National Strategic Plan for Non-Communicable Disease 2016–2025 [4]. Malaysia, the prevalence of tobacco usage has fallen from an estimated 29.6% in 2000 to 24.7% in 2005 and 2010 to 22.8% in 2015. It is anticipated to fall even further to 21% in 2020 and 19.6% in 2025 [4].

Nicotine has a lethal dosage of 40–60 mg or 0.8–1.0 mg.kg⁻¹ body weight of an adult person [5]. Smokers and non-smokers exposed to second-hand smoke have nicotine in their bodily fluids [6]. A small dosage of nicotine does stimulate the central nervous system, which caused arousal, indicators of arousal include an uptick in mood and attention, a boost in energy, and a sense of pleasure [5]. Excessive nicotine intake can lead to serious health effects. Nicotine addiction is shown in a repetitive behaviour on wanting to inhale the vaporized e-cigarette solution. Nicotine addiction in long term would affects the central nervous system, leading to fatal lung disease, chronic obstructive pulmonary disease (COPD), infertility, cancer, vascular disease, and neurodegenerative diseases, such as Parkinson's and Alzheimer's [7]. When our bodies are exposed to nicotine, they will release the adrenaline hormone stimulated by the adrenal glands. Consequently, the adrenaline chemicals will increase our heart rate, blood pressure, and breathing activities. Moreover, nicotine will cause the release of dopamine hormones, where it is a hormone that gives a pleasurable sensation to our brain. It has a similar effect when people consume heroin and cocaine.

Technology has progressed over time, and so has the way individuals use tobacco products.

Manufacturers have recently sought to decrease the amount of carbon monoxide (CO), benzene (C₆H₆), and formaldehyde (CH₂O) in tobacco smoke inhaled, in addition to nicotine. E-cigarettes, which vaporises a particular liquid breathed by the vapers, have replaced cigarette smoking with various nicotine delivery products. Vapers are people who use e-cigarettes. E-cigarettes have many benefits that may assist those who are addicted to traditional cigarettes in trying to quit smoking. However, the long-term use could still be harmful [8]. E-cigarettes contains a wide range of liquids that many people find interesting to consume; propylene glycol (C₃H₈O₂), glycerol (C₃H₈O₃), and aroma are the components of the critical fluid. The maximum dosage of nicotine in e-cigarette liquids is 20 mg.mL⁻¹ in a container with an entire volume of 10 ml, according to the European Union Tobacco Products Directive. The development of novel nicotine determination methodologies appears crucial and necessary in commercial e-cigarette product development.

Nicotine detection is critical in medicine, toxicological research, and forensic science [5]. Conventional techniques have been used to detect nicotine in the liquid phase, such as gas chromatography/mass spectrometry (GC-MS), electrochemiluminescent/flow injection analysis, high-performance liquid chromatography (HPLC), liquid chromatography/mass spectrometry (LC-MS), and atomic absorption spectrometry (AAS) [1]. These traditional techniques have limitations, such as the need for a complex sample pre-treatment procedure, a more extended analysis time, a skilful individual to conduct the instruments, expensive equipment, and a lack of selectivity and sensitivity. As a growing analytical chemistry technology, electrochemical sensors have been widely used among researchers due to their numerous advantages, such as simplicity, robustness, reliability, good selectivity, fast, and relatively overly sensitive detection [9].

An electrochemical sensor may be altered to suit several applications and analytes and accomplish a variety of improvements because of its portability, flexibility, and simplicity. Yu et al. (2020) developed an electrochemical pre-treatment that improved the response to nicotine on AuNPs-SPCE for a mobile electrochemical workstation that is superior for on-the-spot detection [10]. The sample was obtained from 60 different sampling stations in China and representatives from other nations, where they employed a disposable SPE system that consisted of a working gold electrode with a diameter of 4 mm, platinum as a counter electrode, and silver as a reference electrode.

Many carbon-based sensors for nicotine detection have been modified with nanoparticles, such as electro-reduced carboxylate graphene [11] nano-carbon [2], multi-wall carbon nanotubes and nitrogen-doped graphene sheets (NGS) were produced

by Li et al., (2016) [12]. Li et al., (2016) also investigated on nicotine electrochemistry on a multi-walled carbon nanotube-alumina-coated silica (MWCNT/ACS) nanocomposite electrode using an irreversible reduction peak on a glassy carbon electrode modified with MWCNT. Nicotine's high overpotential on carbonic electrode material has been addressed by Suffredini 2005 that was developed using Boron-Doped Diamond Electrode [13]. The detection was reported on a vast working potential range, a low and constant background stability, and a low bias for adsorption. The authors also proposed a mechanism for nicotine oxidation in an alkaline environment based on semi-empirical calculations; however, this process has not yet been verified.

This work created new prospects for the widespread use of carbon-based electrodes. Gold nanoparticles were modified on carbon surface using electrodeposition method due to sluggish carbon electrode kinetics and response happening at highly positive and negative potentials. Since, the specific redox determination for target analyte (nicotine) is constrained by the electrode material's potential range at its anodic/cathodic ends, overlapping with oxygen and hydrogen evolution potential areas that often resulted in unreproducible findings. To address the main issue of nicotine's significant overpotential on bare SPCE, electrode surface modifications have been made by electrodeposition of gold nanoparticles on the SPCE to enhance the electroactivity of nicotine.

EXPERIMENTAL

1. Materials

Screen-printed carbon electrode (SPCE) is a 3-in-1 electrode consisting of the working electrode (carbon), counter electrode (carbon), and reference electrode (silver) bought from Metrohm DropSens; whereas the screen-printed gold electrode (SPGE) using gold as working electrode was purchased from Dropsens, Netherlands.

2. Chemicals

Tetrachloroauric(III) acid trihydrate ($\text{HAuCl}_4 \cdot 3\text{H}_2\text{O}$), potassium ferrocyanide ($\text{K}_4\text{Fe}(\text{CN})_6 \cdot 3\text{H}_2\text{O}$), sulphuric acid (H_2SO_4), and nicotine ($\text{C}_{10}\text{H}_{14}\text{N}_2$) were purchased from Sigma Aldrich, Germany.

3. Instruments

Autolab Potentiostat (Metrohm, Netherlands) interfaced with Nova 11.1. were used for electrochemical characterisation and measurements.

4. Nicotine Samples

The samples used in this experiment are e-cigarettes' liquid from Sober Supplies with different aromas (flavourings and sweeteners), and other ingredients

(vegetable glycerine and propylene glycol) bought from shops that sell e-cigarettes' liquid in Shah Alam, Malaysia. A standard nicotine solution at $1.010 \text{ g}\cdot\text{mL}^{-1}$ (Sigma-Aldrich) was prepared by diluting the commercial standard solution in 0.1 M phosphate-buffered saline (PBS) at pH 7 to envisage future application of nicotine detection from body fluid such as from saliva and urine sample.

5. Methods

5.1. Electrochemical Pre-treatment on SPCE

SPCE needs to undergo a pre-treatment process to prevent the carbon surface from any contaminants and to enhance the electron transfer on the working electrode of the SPCE. The SPCE was rinsed with the distilled water and then the SPCE has undergoes a cleaning process via cyclic voltammetry (CV) by applying -0.5 V to $+2.0 \text{ V}$ potential range at a scan rate of $100 \text{ m}\cdot\text{Vs}^{-1}$ in $1.0 \text{ M H}_2\text{SO}_4$ solution. Cleaned SPCE is ready to use for electrochemical deposition and measurements. All electroanalysis were carried out in triplicate.

5.2. Preparation of HAuCl_4 Solution

The $\text{HAuCl}_4 \cdot 3\text{H}_2\text{O}$ powder was weighed at approximately 0.39 g to prepare 10 mM of HAuCl_4 solution. The gold tetrachloride powder was homogeneously diluted in a 100-mL volumetric flask with 6 mL of $96\% \text{ H}_2\text{SO}_4$ solution.

5.3. Synthesis of Gold Nanoparticles (AuNPs) Modified SPCE

All three-system SPCEs were immersed in the prepared gold solution for deposition of gold nanoparticles (AuNPs) on the SPCE working electrode. The counter electrode was used to close the current circuit, and the reference electrode was used to provide the stable potential for controlled regulation of working electrode potential. The selective potential range for the electro-deposition of AuNPs on SPCE was obtained using CV at a potential of $+0.53 \text{ V}$. Then, chronoamperometry (CA) method was applied at a constant potential of -0.9 V for 900 seconds. The effect of deposition potential and deposition time on the formation of AuNPs on SPCE was studied, where this process was conducted at room temperature. The synthesised AuNPs on the working electrode were rinsed with distilled water and dried in a nitrogen stream to dry the modified SPCE surface. The fabricated AuNPs-SPCE was ready to be used for further measurements.

5.4. Analysis of $[\text{Fe}(\text{CN})_6]^{3-/4-}$ in 0.1 M KCl

The $[\text{Fe}(\text{CN})_6]^{3-/4-}$ solution was used as an electrolyte to be analysed using CV by applying -0.2 V to $+0.6 \text{ V}$ potential range at a scan rate of $100 \text{ mV}\cdot\text{s}^{-1}$. To evaluate SPCE, SPGE, and AuNPs-SPCE electrochemical performance the rest of the concentrations

0.00001 M, 0.0001 M, 0.001 M, 0.01 M, and 0.1 M of $[\text{Fe}(\text{CN})_6]^{3-/4-}$ solution was prepared by using dilution method $M_1V_1 = M_2V_2$ from the 0.1 M of $[\text{Fe}(\text{CN})_6]^{3-/4-}$ in 0.1 M KCl.

5.5. Preparation of Standard Nicotine in 0.1 M PBS (pH 7) Solution

A standard nicotine solution of 80.31 μl was diluted with 0.1 M phosphate-buffered saline (PBS) at pH 7 to prepare 0.05 M nicotine standard stock solution. Series of nicotine standards solutions were then prepared using the dilution method to produce different concentrations ranging from 0.00025 M to 0.03 M.

5.6. Nicotine in E-cigarette Solution Detection

Approximately 15 μL of commercial e-cigarette that was labelled by the manufacturer as having 50 mg nicotine in 30 mL of e-cigarette packaging (container) was directly dropped and tested on the AuNPs-SPCE to observe the redox reaction that had occurred. Subsequently, 1.5 ml of the flavoured of e-cigarettes was spiked into the test solution to validate the electrochemical nicotine detection.

6. Characterisation of AuNPs-SPCE Surface Morphology

6.1. Scanning Electron Microscope (SEM)

Field emission scanning electron microscope (FESEM Carls Zeiss SMT Supro 40VP, ETH 5 kV) was used to study the surface morphology of the deposited AuNPs-SPCE at 1500 \times magnification.

6.2. Energy Dispersive X-ray Spectroscopy (EDX)

Energy Dispersive X-Ray Spectroscopy (EDX control software Oxford INCA X-max 51-XXM 0021 equipped with FESEM, ETH 10 kV) was used for determination of chemical composition of SPCE electrode and modified SPCE with gold nanostructures.

RESULTS AND DISCUSSION

1. Electrochemical Behaviour of Pre-treated SPCE

Figure 2 shows cyclic voltammograms obtained from the SPCE before and after electrochemical pre-treatment in 1.0 M H_2SO_4 aqueous solution at a sweep rate of 100 $\text{mV}\cdot\text{s}^{-1}$. H_2SO_4 was used as supporting electrolyte because as compared to other acids, H_2SO_4 provides sufficient ionic conductivity which resulted in huge density of proton in the electrolyte media. During the anodic scan, an oxidation peak was observed at a potential around +0.5 V on detection of 0.1 M $[\text{Fe}(\text{CN})_6]^{3-/4-}$ for SPCE that underwent electrochemical pre-treatment, whereas no oxidation peak was obtained for untreated SPCE. The detecting effects of the electrode after pre-treatment were determined to be better than the untreated SPCE with a considerable rise in current [10].

2. Effect on Types of Electrodes

The electrochemical behaviour of the AuNPs-SPCE was compared with SPCE and SPGE using CV in a 0.1 M KCl + 0.01 M $[\text{Fe}(\text{CN})_6]^{3-}$ at the applied potentials, -0.2 V and +0.6 V at a scan rate of 100 $\text{mV}\cdot\text{s}^{-1}$. As shown in Figure 3, the SPCE has well-

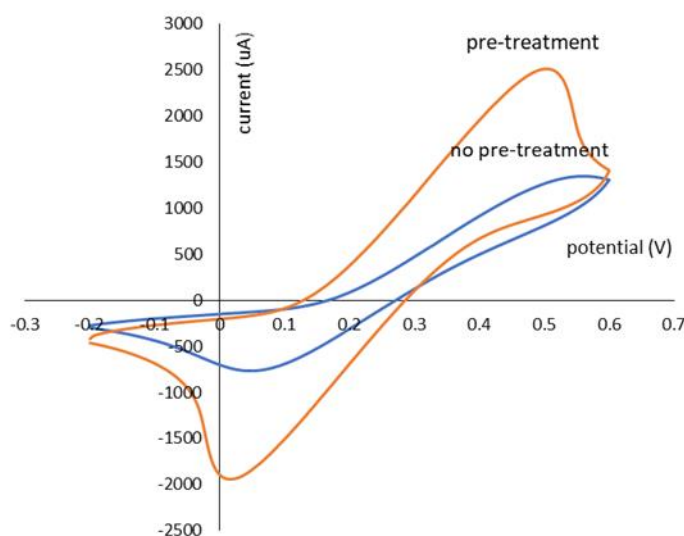


Figure 2. Cyclic voltammograms of untreated SPCE (blue) and treated SPCE (orange) in a 0.1 M KCl containing 0.1 M $[\text{Fe}(\text{CN})_6]^{3-}$ solution.

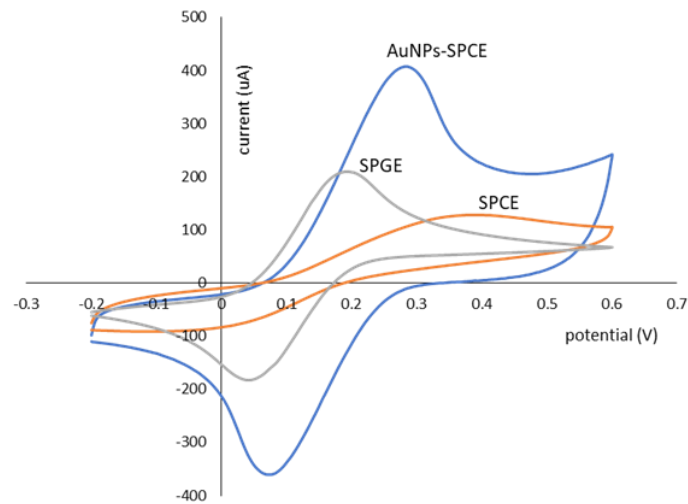


Figure 3. Cyclic voltammograms for SPCE (blue), SPGE (orange), AuNPs-SPCE (grey) in 0.01 M of $[\text{Fe}(\text{CN})_6]^{3-}$ in 0.1 M KCl solution at scan rate $100 \text{ mV}\cdot\text{s}^{-1}$.

defined redox peaks: E_{pa} (oxidation peak) at potential $+0.39 \text{ V}$ and E_{pc} (reduction peak) at potential $+0.01 \text{ V}$, while the SPGE has redox peaks: E_{pa} at potential $+0.2 \text{ V}$ and E_{pc} at potential $+0.015 \text{ V}$ than SPCE. Specifically, the redox peaks of AuNPs-SPCE at E_{pa} at potential $+0.3 \text{ V}$ and E_{pc} at potential $+0.1 \text{ V}$. The results indicated that modification of SPCE with AuNPs-SPCE has significantly enhanced the electroconductivity of SPCE and subsequently increased the redox current that had occurred in the measurement of the SPCE [14]. It can be observed that SPGE has lower oxidation peak response, compared to the AuNPs-SPCE, suggesting that modification of the modified SPCE resulted in higher electrochemical active surface area (ECSA) as compared to SPGE.

3. Effect of Scan Rate on $[\text{Fe}(\text{CN})_6]^{3-}$ Redox Behaviour on AuNPs-SPCE

Figure 4 shows the CV of the AuNPs-SPCE electrode

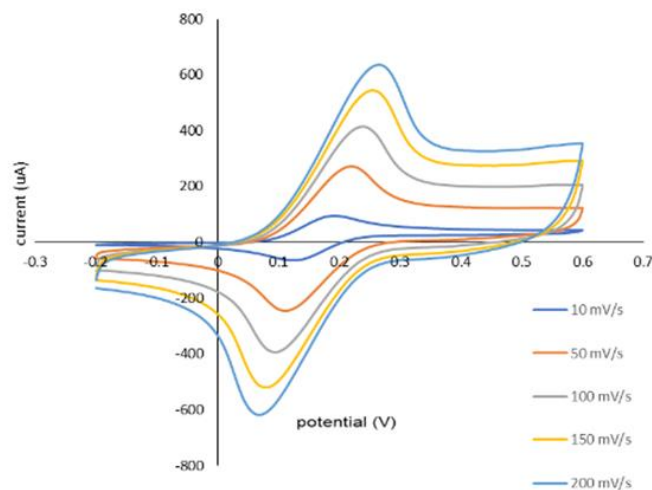


Figure 4. Cyclic voltammograms of AuNPs-SPCE prepared at -0.9 V in $0.01 \text{ M } [\text{Fe}(\text{CN})_6]^{3-}$ in 0.1 M KCl solution at different scan rates.

that was immersed in 0.1 M KCl containing $0.01 \text{ M } [\text{Fe}(\text{CN})_6]^{3-}$ scanned at various scan rates from $10 \text{ mV}\cdot\text{s}^{-1}$ to $200 \text{ mV}\cdot\text{s}^{-1}$. The findings demonstrated greater peak currents with increased scan rate. This indicates that the current response for an adsorbed species is expected to be a free diffusing species, deviation from the peak of current versus the scan rate. Elgrishi et al., (2018) suggested that electron transfer may be occurring via surface-adsorbed species. From the cyclic voltammograms, each of the scan rates shows similar CV profiles, in which both peaks I_{pa} (oxidation peak) and I_{pc} (reduction peak) were enhanced as the scan rate increased [15]. The peak potentials are slightly shifted to a more positive potential for E_{pa} (oxidation potential) and more negatively for E_{pc} (reduction potential) with increasing scan rates.

The redox trend of the $[\text{Fe}(\text{CN})_6]^{3-}$ on AuNPs-SPCE was investigated by plotting a graph of the scan rate ($\text{mV}\cdot\text{s}^{-1}$). In these electrochemical experiments,

the scan rate was used to control how fast the applied potential is scanned using an AuNPs-SPCE. The scan rate is inversely proportional to the size of the diffusion layer, which we can observe higher currents in the analysis. Cyclic voltammetry of $[\text{Fe}(\text{CN})_6]^{3-/4-}$ was electrochemically reversible with electron transfer processes involving freely diffusing redox species. Randles-Sevcik (Equation 1) provides indications of the analyte is freely diffusing in the probe solution, where the peak current i_p (A) increases linearly with the square root of the scan rate v ($\text{V}\cdot\text{s}^{-1}$), n is the number of electrons transferred in the redox reaction, A (cm^2) is the electrode surface area, D_0 ($\text{cm}^2\cdot\text{s}^{-1}$) is the diffusion coefficient of the oxidised analyte, and C° ($\text{mol}\cdot\text{cm}^{-3}$) is the bulk concentration of the analyte.

$$i_p = 0.446nFAC^\circ \left(\frac{nFvD_0}{RT}\right)^{1/2} \quad (1)$$

From Figure 5, it is evident that AuNPs-SPCE exhibited excellent linearity with a high correlation of $R^2 = 0.9533$, indicating the $[\text{Fe}(\text{CN})_6]^{3-}$ oxidation occurred on the nanogold coating electrode is a diffusion-controlled process. Elgrishi et al. (2018) suggested that electron transfer may occur via surface-adsorbed species. Au nanostructure interconnectivity resulting highly in conductive network that makes electrons to be transported easily.

4. Surface Characterisation of AuNPs-SPCE

4.1. Surface Morphology of AuNPs-SPCE

The applied potential used for the deposition is an

important factor in controlling the morphologies and structure of AuNPs. Scanning Electron Microscope (SEM) was used performed to investigate the variable of electrodeposition potential on the AuNPs-SPCE morphology on SPCE that have been electrodeposited under different applied potentials, which is the first layer of gold nanoparticles at +0.53 V and the second layer of gold nanoparticles at -0.9 V for 900s from 10 mM HAuCl_4 solution.

Additionally, the SEM was used to capture the image of bare SPCE and to observe the SPCE's surface changes before and after the deposition of AuNPs on the SPCE. The surface of carbon on SPCE consists of uneven gold nanoparticles with spiky looks (Figure 6a). In the first layer deposition of gold nanoparticles, the potential was applied at +0.53 V by using CA (Figure 6b). The nanogold coating effectively coated the bare carbon of SPCE, which is composed of quasi-spherical-like and faceted nanostructures scattered on the SPCE surface with particle smaller sizes. However, owing to the low current of the first gold nanoparticle deposition, which restricts the crystallisation and development of gold nanostructure, the gold coating did not completely cover the SPCE surface. Due to diffusion-limited conditions, the second gold nanoparticles were electrodeposited at -0.9 V by using CA (Figure 6c), resulting in some larger dendrite-like gold nanoclusters with several micrometres of gold nanostructures, as an example of the sufficiently negative applied potential in electrodeposition. Figure 10c shows the formation of a dense and rough gold structure with huge micrometres of gold nanostructures and feather-like branches on the SPCE when deposited at -0.9 V in the presence of the hydrogen evolution process.

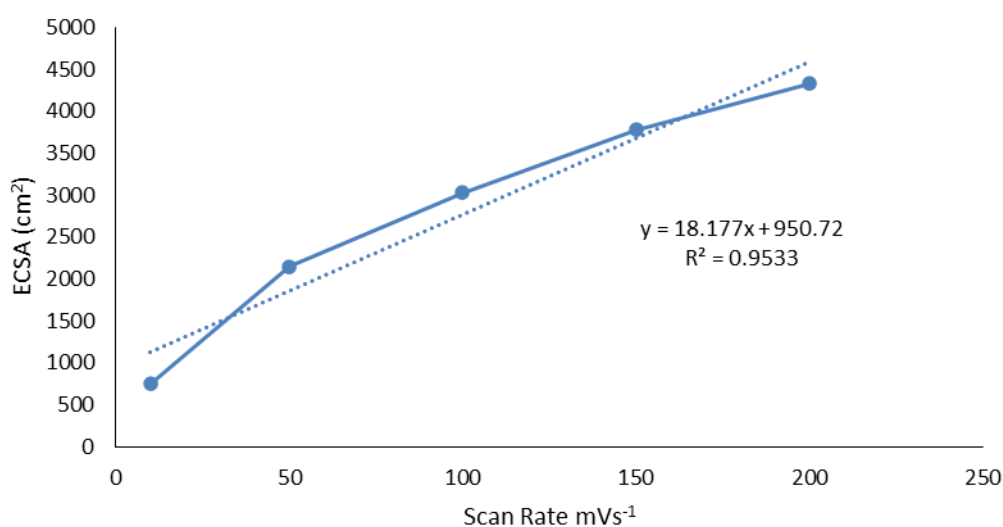


Figure 5. The effect of scan rate towards ECSA of AuNPs-SPCE using 0.01 M $[\text{Fe}(\text{CN})_6]^{3-}$ in 0.1 M KCl solution.

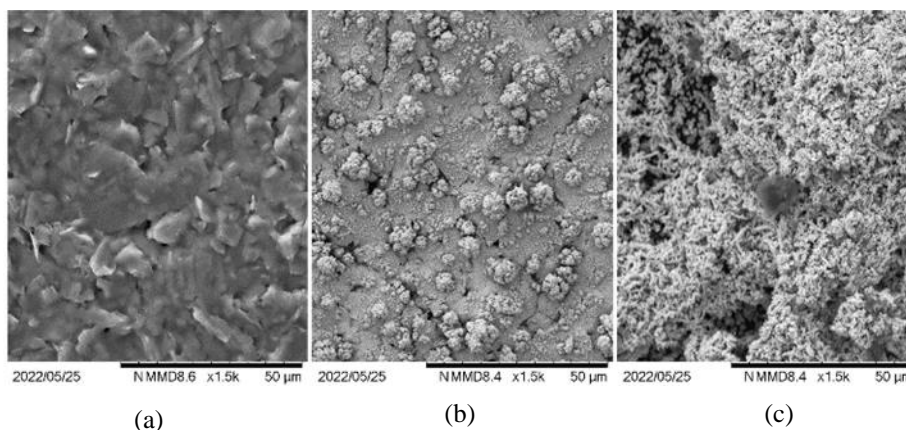


Figure 6. SEM images of gold nanostructure prepared from 10 mM HAuCl₄: (a) bare SPCE and gold nanostructures on SPCE deposited at: (b) +0.53 V (underlayer gold coating); and (c) -0.9 V (second gold coating) for 900s. The magnification is at 1500 \times .

Table 1. The elemental composition of gold nanostructures coating prepared at different deposition potentials

Deposition Potential (V)	Surface Composition (Weight (wt.%))		
	Au	O	C
+0.53	97.09	2.91	ND
-0.9	97.21	2.79	ND

ND = Not Detected

4.2. Energy Dispersive X-ray Spectroscopy (EDX) Analysis of AuNPs-SPCE

Table 1 shows the elemental compositions of gold nanostructures electrodeposited on SPCE prepared at various deposition potentials. Analysis of the underlayer gold coating prepared at +0.53 V about 97.09 wt.% of gold (AuNPs) present. The amount of carbon (C) was undetected, as shown by SEM in Figure 6b,

in which the second gold coating was almost coated. The AuNPs amount of gold was detected was 97.21 wt.% for the second layer of gold nanoparticles deposition at -0.9 V with the low amount of oxide formed and the absence of the C element suggested that AuNPs were fully deposited on the surface of the substrate. S peak was not detected because SO₄²⁻ did not react on the working electrode within the potential scanned.

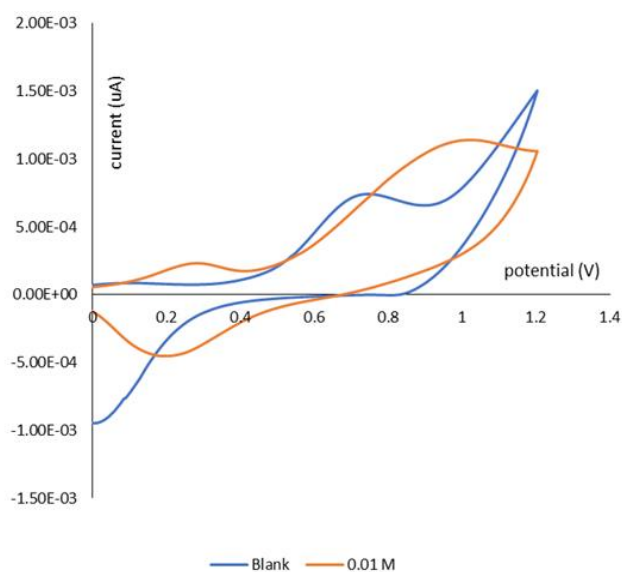


Figure 7. Cyclic voltammograms obtained at the AuNPs-SPCE in the absence of nicotine (blank) (blue) and in the presence of 0.01 M nicotine oxidation peak at +0.2 V in 0.1 M PBS (pH 7) (orange) at a scan rate of 100 mV.s⁻¹.

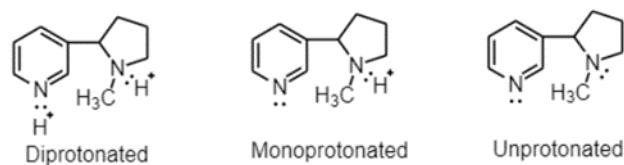


Figure 8. Structures of nicotine in water with different forms: diprotonated (acid), monoprotated (neutral), and unprotonated (basic) [16].

5. Cyclic Voltammetry Analysis of Standard Nicotine on AuNPs-SPCE

Cyclic voltammetry (CV) was employed to study the electrochemical behaviour of nicotine on AuNPs-SPCE. Figure 7 shows the corresponding voltammograms in the absence of nicotine (Blank, 0.1 M PBS, pH 7) and in the presence of 0.01 M nicotine in 0.1 M PBS (pH 7) on AuNPs-SPCE. Following many other investigations during the anodic scan, nicotine undergoes electrochemical oxidation at potential +0.25 V and no oxidation peak current for blank when nicotine was absent in the blank solution. During the cathodic scan that was reversed at potential +1.2 V, the voltammogram showed a reduction peak of nicotine at around +0.2 V as well. No such peak was observed in the blank solution of void nicotine. The redox current peak of each nicotine in this experiment observed oxidation and reduction peaks at +0.25 V and +0.2 V, respectively.

6. Effect of pH in nicotine detection on AuNP-SPCE

Upon nicotine dissolution in aqueous solution, it can exist in one of three forms, depending on the pH of the solution: unprotonated (basic), monoprotated (neutral), and diprotonated (acid), as shown in Figure 8.

The redox behaviour of these nicotine solutions was electrochemically observed using CV at an applied potential range from -1.0 V to +1.0 V and a scan rate of 100 mV.s⁻¹. Figure 9 (a-c) shows CV profiles of nicotine in the effect of pH. The unprotonated forms resulted in the oxidation of nicotine at +0.55 V. Then, 0.1 M HCl was

added to 0.05 M nicotine (pH 10) to achieve a pH of 5, in which it exists as a diprotonated species. Figure 9(b) shows the CV profile of 0.05 M nicotine (pH 5), which shows that nicotine can be observed at around +0.2 V. Phosphate-buffer saline (0.1 M PBS, pH 7) was used as the solvent in preparation of 0.05 M stock nicotine solution. This is because nicotine exists as a monoprotated compound in the pH of physiological body fluid. Meanwhile, Figure 9(c) illustrates oxidation and the peaks of oxidation, as observed via the cyclic voltammetry at potential +0.25 V.

7. Detection of Nicotine in E-cigarettes on AuNPs-SPCE

According to The Centers for Disease Control and Prevention (CDC), the amount of nicotine required for a lethal dose on an adult is approximately 30–60 mg [17]. In this experiment, the AuNPs-SPCE was used to detect nicotine in liquid flavouring in e-cigarettes by using cyclic voltammetry (CV). Various concentrations of standard nicotine in 0.1 M PBS (pH 7), which were from 0.00025 M to 0.03 M were performed using CV at the potential range -0.9 V to +1.2 V at the scan rate 100 mV.s⁻¹ on AuNPs-SPCE to study the electrochemical behaviour of nicotine redox reaction. Figure 10 inset shows that 0.00025 M of nicotine can be detected on the CV by using the AuNPs-SPCE, which has a redox reaction potential of: E_{pa} at +0.26 V and E_{pc} at -0.24 V. The higher the concentration of nicotine, the higher the redox peaks observed on the CV, signifying that the AuNPs-SPCE contributes to acceptable sensitivity and selectivity to the detection of nicotine.

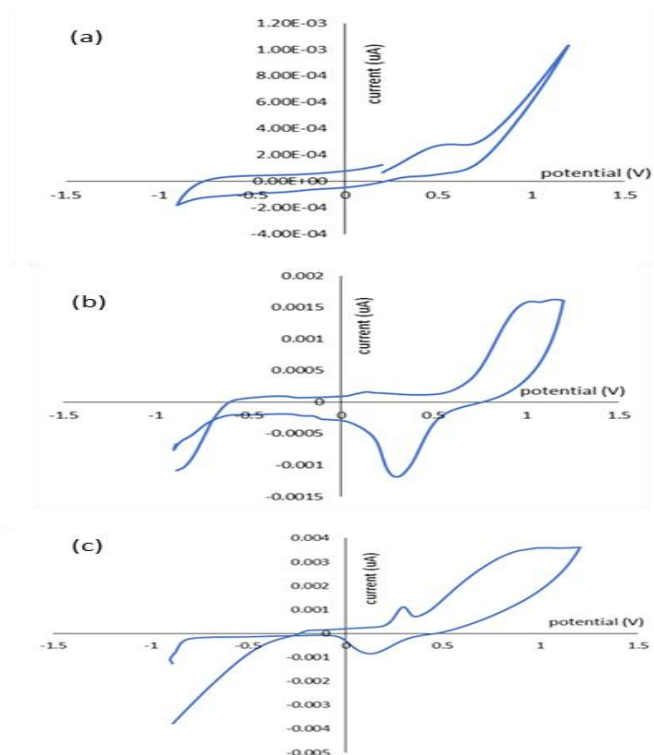


Figure 9. Cyclic voltammograms of: (a) AuNPs-SPCE of 0.05 M nicotine in de-ionized water (pH 10) (unprotonated forms, basic); (b) 0.05 M nicotine in de-ionized water (pH 5) (diprotonated forms, acidic); and (c) 0.05 M nicotine in 0.1 M PBS (pH 7) (monoprotonated forms, neutral).

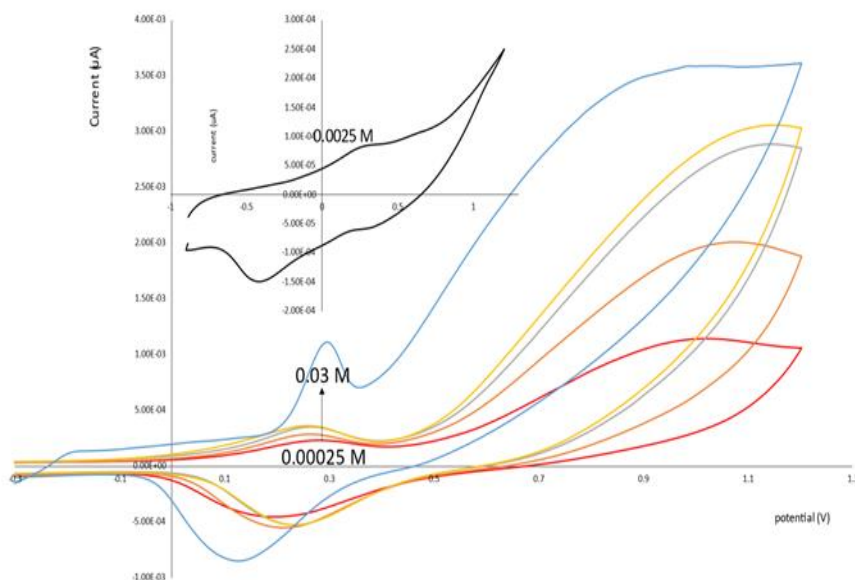


Figure 10: Cyclic voltammograms of AuNPs-SPCE in 0.1 M PBS (pH 7) at various concentrations of nicotine. Inset top; voltammogram for 0.00025 M nicotine.

Figure 11 shows the plot of the current (μA) versus the concentration of nicotine (M). It is evident from the plot of current (μA) versus concentration of nicotine (M) that AuNPs-SPCE exhibited excellent

linearity with a high correlation of $R^2 = 0.9920$ ($n = 3$), indicating that the occurrence of nicotine oxidation on the gold coating electrode is a diffusion-controlled process at concentration between 0.00025 M and 0.03 M.

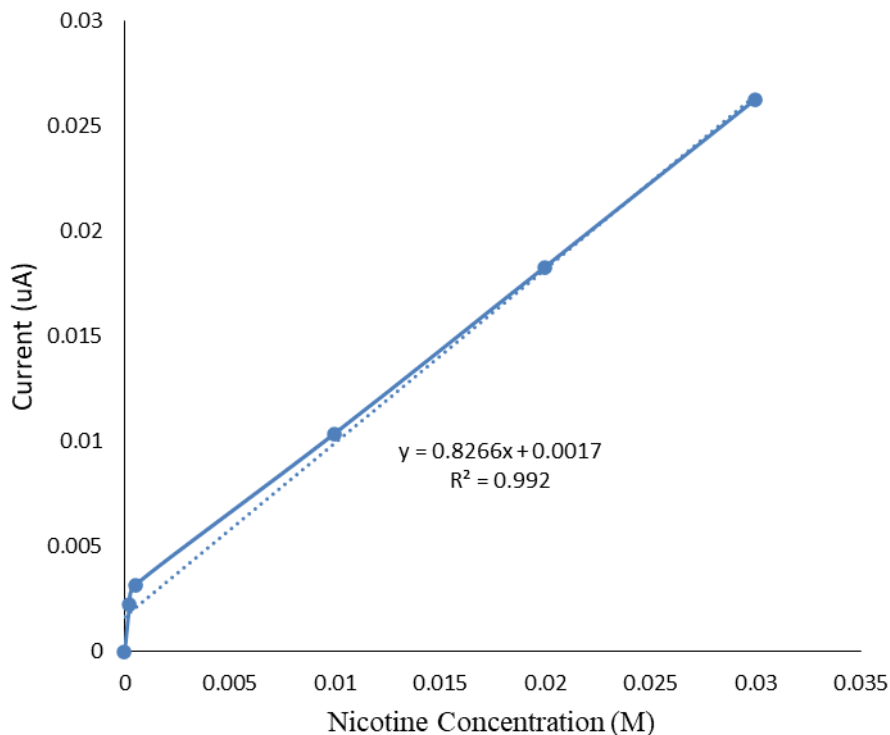


Figure 11. The typical calibration curve of various nicotine concentrations in 0.1 M PBS (pH 7) on AuNPs-SPCE at potential +0.2 V and scan rate of 100 mV.s⁻¹.

8. Interference Study on Nicotine in E-cigarette Solution

The e-cigarette sample was manufactured by Sober Supplies (Malaysia) that consisted of a liquid flavoured e-cigarette solution. The other ingredients or chemical compositions disclosed in the liquid flavour by the manufacturer are vegetable glycol (glycerine), and

propylene glycol. This study included investigation on the interference of these compounds in the 0.05 M nicotine in 0.1 M PBS (pH 7) added with the 0.03 M glycerol and 0.03 M Di-propylene glycol, respectively. On the other hand, Figure 12 demonstrates the absence of distinctive redox peak for each of the interference compounds, signifying that the compounds did not affect the redox reaction of the nicotine at potential +0.2 V.

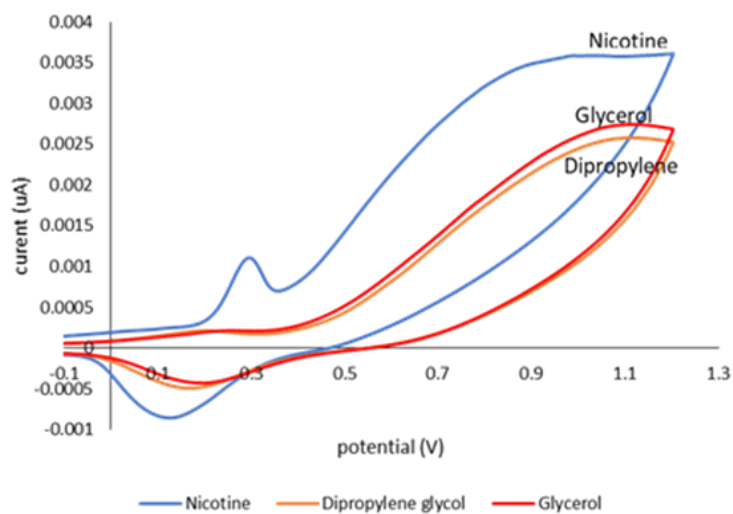


Figure 12. Cyclic voltammograms of AuNPs-SPCE on the 0.05 M nicotine (blue), 0.03 M Di-propylene glycol (orange) and 0.03 M glycerol (red) 0.1 M PBS (pH 7) PBS.

Table 2. The reported electrochemical methods for nicotine determinations.

Type of sample	Analytical technique	Limit of detection	Year of publication	References
Human urine	Amperometric using CuWO ₄ /Rgo/Nf immobilised GCE	0.035 μM	2019	[18]
Liquid for e-cigarettes	Amperometric using CuHCF-PPy	0.03 mM	2019	[19]
Liquid for e-cigarettes	DPV using BDDE	0.06 M	2019	([5])
Liquid for e-cigarettes	CV using AuNPs-SPCE	0.0008 M	2022	This work

CONCLUSIONS

Nicotine has been successfully detected using AuNPs-SPCE in this work. The electrochemical deposition of gold nanoparticles on the SPCE surface were investigated using cyclic voltammetry and chronoamperometry techniques. The surface properties of gold nanoparticles applied to SPCE demonstrated the impact of the deposition potential. Gold nanoparticles (AuNPs) that were electrodeposited at different potentials produced various morphologies of gold nanostructures. The ECSA of gold nanoparticles deposited at potential -0.9 V of AuNPs-SPCE is superior to commercial SPGE for nicotine detection. CV was also used to investigate the electrochemical detection of nicotine using AuNPs-SPCE. It was discovered that the AuNPs-SPCE having compatible performances for nicotine when compared to earlier studies (Table 2). The calibration graph was linear from 0.00025 M to 0.03 M, with a correlation (R^2) of 0.9920 and a limit detection of 0.00083 M ($S/N = 3$). The preliminary results might be used for ongoing nicotine content monitoring in commercially available e-cigarette liquids.

In this study, the narcotic substance of tobacco products in e-cigarette were detected using the modified AuNPs-SPCE. This discovery will significantly benefit the community, particularly health care providers in the detection of nicotine addiction among patients and avoiding deadly overdoses of nicotine.

ACKNOWLEDGEMENT

This work was supported by the Ministry of Education (MOE) through Fundamental Research Grant Scheme (FRGS/1/2021/TK0/UIAM/02/9).

REFERENCES

- Mehmeti, Eda, Kilic, T., Laur, C., Carrara, S., Polytechnique, É., Lausanne, F. De & Systems, I. (2020) Electrochemical determination of nicotine in smokers' sweat. *Microchemical Journal*, **158**, 105155.
- Shehata, M., Azab, S. M., Fekry, A. M. & Ameer, M. A. (2016) Nano-TiO₂ modified carbon paste sensor for electrochemical nicotine detection using anionic surfactant. *Biosensors and Bioelectronics*, **79**, 589–592.
- Domenico Bonamonte¹, M. D., M. V. (2016) Tobacco Induced Contact Dermatitis. *European Journal of Dermatology*, **26(3)**, 223–231.
- World Health Organisation (2019) WHO global report on trends in prevalence of tobacco use third edition, World Health Organisation.
- Kowalcze, M., Jakubowska, M., (2020) Voltammetric determination of nicotine in electronic cigarette liquids using a boron-doped diamond electrode (BDDE). *Diam. Relat. Mater.*, **103**, 107710.
- Events, A. C. (2010) Secondhand Smoke Exposure and Cardiovascular Effects. In *Secondhand Smoke Exposure and Cardiovascular Effects*. Institute of Medicine (US) Committee on Secondhand Smoke Exposure and Acute Coronary Events. Washington (DC): National Academies Press (US), Available from: <https://www.ncbi.nlm.nih.gov/books/NBK219565/> doi: 10.17226/12649
- Jerome, R. & Sundramoorthy, A. K. (2020) Preparation of hexagonal boron nitride doped graphene film modified sensor for selective electrochemical detection of nicotine in tobacco sample. *Analytica Chimica Acta*, **1132**, 110–120.
- Sobieski, E., Yingst, J. and Foulds, J (2022) Quitting electronic cigarettes: Factors associated with quitting and quit attempts in long-term users. *Addictive Behaviors*, **127**, 107220.
- Bekmezci, M., Bayat, R., Erduran, V. & Sen, F. (2022) Biofunctionalization of functionalized nanomaterials for electrochemical sensors. *Functionalized Nanomaterial-Based Electrochemical Sensors: Principles, Fabrication Methods,*

- 12 Amirul Aiman Ali Amran, Lim Ying Chin, Nurasyiqin Azman, Nurfadhilah Jafar, Yusairie Mohd, Rosminazuin Ab Rahim, Anis Nurashikin Nordin, Zainiharyati Mohd Zain and Applications, *1st Edition, Elsevier, UK*, 55–69.
10. Yu, C., Yu, J., Zhang, H., He, Z., Sha, Y., Liu, B., Wang, Y., (2020) A facile approach for rapid on-site screening of nicotine in natural tobacco. *Environ. Pollut.*, **259**, 113841.
11. Li, X., Zhao, H., Shi, L., Zhu, X., Lan, M., Zhang, Q. & Hugh Fan, Z. (2017) Electrochemical sensing of nicotine using screen-printed carbon electrodes modified with nitrogen-doped graphene sheets. *Journal of Electroanalytical Chemistry*, **784**, 77–84.
12. Li, H., Wang, W., Lv, Q., Xi, G., Bai, H., Zhang, Q. (2016) Disposable paper-based electrochemical sensor based on stacked gold nanoparticles supported carbon nanotubes for the determination of bisphenol A. *Electrochem. commun.*, **68**, 104–107.
13. Suffredini, H. B., Santos, M. C., De Souza, D., Codognoto, L., Homem-de-Mello, P., Honório, K. M., da Silva, A. B. F., Machado, S. A. S. & Avaca, L. A. (2005) Electrochemical Behavior of Nicotine Studied by Voltammetric Techniques at Boron-Doped Diamond Electrodes. *Analytical Letters*, **38(10)**, 1587–1599.
14. Wu, J., Pil, J., Dooley, K., Cropek, D. M., West, A. C., Banta, S., (2011) Rapid Development of Gold Nanoparticle Deposited on Screen-Printed Carbon Electrode for Electrochemical Detection of Nicotine in E-cigarette
- New Protein Biosensors Utilizing Peptides Obtained via Phage Display. **6(10)**, 1–9.
15. Elgrishi, N., Rountree, K. J., McCarthy, B. D., Rountree, E. S., Eisenhart, T. T., Dempsey, J. L. (2018) A Practical Beginner's Guide to Cyclic Voltammetry. *J. Chem. Educ.*, **95**, 197–206.
16. Borgerding, M. F., Perfetti, T. A., Ralapati, S. (1999) Determination of nicotine in tobacco, tobacco processing environments and tobacco products. *Anal. Determ. Nicotine Relat. Compd. their Metab.*, **285–391**. <https://doi.org/10.1016/B978-044450095-3/50010-3>.
17. Mayer, B. (2014) How much nicotine kills a human? Tracing back the generally accepted lethal dose to dubious self-experiments in the nineteenth century. *Arch. Toxicol.*, **88**, 5–7.
18. Karthika, A., Karuppasamy, P., Selvarajan, S., Suganthi, A., Rajarajan, M. (2019) Electrochemical sensing of nicotine using CuWO₄ decorated reduced graphene oxide immobilized glassy carbon electrode. *Ultrason. Sonochem.*, **55**, 196–206.
19. Lee, P. K., Woi, P. M. (2019) Direct self-assembly of CuHCF-PPy nanocomposites on rGO for amperometric nicotine sensing at high concentration range. *J. Electroanal. Chem.*, **837**, 67–75.